Met. Mater. Int., Vol. 16, No. 1 (2010), pp. 77~81
Doi: 10.1007/s12540-010-0077-9 Published 26 February 2010

SnO_2-Core/SiO_x-Shell Coaxial Whiskers with a Needle-Like Morphology

Hyoun Woo Kim*, Hyo Sung Kim, MesfinAbaynehKebede, Han Gil Na, and Ju Chan Yang

School of Materials Science and Engineering, Inha University,
Incheon 402-751, Korea

(received date: 19 December 2008 / accepted date: 5 August 2009)

Needle-shaped structures of tin oxide (SnO_2) were coated with a shell layer of SiO_x via a sputtering method.The diameters of the SiO_x-coated structures gradually became thinner, leading to the formation of sharp tips. The whiskers consisted of a crystalline SnO_2 core surrounded by an amorphous SiO_x shell.The photoluminescence (PL) spectrum with a Gaussian fitting exhibited yellow-green and orange light emission bands, and the overall shape and intensity of the PL spectrum were not changed by the SiO_xcoating. The results of this study suggest that sputtering can be employed to achieve the layered growth of shell layers on a variety of nanostructures.

Keywords: nanostructured materials, chemical synthesis, sputtering, optical properties, transmission electron microscopy (TEM)

1. INTRODUCTION

There has been considerable interest in the growth of a variety of nanostructures for nanodevice applications [1-15]. One of the most interesting and urgent challenges in this area is the fabrication of 1D materials with novel morphologies. Needle-shaped whiskers, which have tips showing a sharp curvature, are expected to be of particular importance not only for scientific interest but also for future industrial applications. For example, they are known to improve the field emission properties significantly [16,17].

Tin dioxide (SnO_2) is a well-known functional material that has been used extensively in dye-based solar cells [18], transparent conducting electrodes [19], and gas sensors [20,21]. Accordingly, there has been intense interest in synthesizing SnO_2 1D nanomaterials [22-25].

In an effort to realize various tailor-made functions, coaxial 1D structures with a core/shell geometry have been studied [26,27]. Moreover, their potential wasrecently demonstrated in nanodevice applications of a field-effect transistor [28,29] and a laser [30]. In particular, the formation of a SiO_x shell offers chemical stability [31], thermal stability [32], insulating characteristics [33], and protection from contamination. It also potentially allows for robust attachment of a variety of specific ligands [34,35], as the SiO_x surface is easily functionalized with various coupling reagents. Furthermore, the SiO_x coating layer is optically transparent for visible absorption/emission and does not degrade the intrinsic optical properties of the core materials [32]. In the present work, the fabrication of coaxial needle-shaped whiskers with a SnO_2 core and a SiO_x shell is reported. The SnO_2 whiskers were coated via a sputtering technique using aSi target as a Si source. In addition, structural and optical characterization was carried out.

*Corresponding author: hwkim@inha.ac.kr

2. EXPERIMENTAL PROCEDURES

Sn powder (purity: 99.9 %) was used as the source material and was placed in a ceramic boat. The boat was put into a quartz tube in a high-temperature furnace.A Ir (about 150 nm-thick)-coated Si plate was situated on top of the ceramic boat with the Ir-coated side downwards, acting as a substrate to collect the growth products. Ambient gas flowed at a constant total pressure of 2 Torr with the percentage of O_2 and Ar partial pressure being set to 3 % and 97 %, respectively. The temperature of the furnace was set to 900 °C for 1 h.

Coating experiments on the as-prepared SnO_2 whiskers were subsequently carried out using a DC turbo sputter coater (Emitech K575X, Emitech Ltd., Ashford, Kent, UK). The sputtering target was a piece of polished p-type (100) Si wafer with a resistivity of 1-30 Ω cm. The wafer was blow-dried under N_2 gas. The distance between the target and the SnO_2 whiskers was approximately 50 mm. With a base pressure of about 2×10^{-4} Pa,sputtering was carried out under Ar plasma at room temperature. The deposition time was in a range of 0.5-2 min with a DC sputtering power of approximately 33 W.

Scanning electron micrographs (SEMs) were taken using a Hitachi S-4200 scanning electron microscope. Glancing angle

(0.5°) X-ray diffraction (XRD) was carried out with a Philips X'pert MRD x-ray diffractometer with CuKα_1 radiation. Transmission electron micrography (TEM) and high-resolution TEM were accomplishedon a Philips CM-200 (200 kV) transmission electron microscope. In addition, the TEM instrument was equipped with an energy-dispersive X-ray spectroscope (EDX). Photoluminescence (PL) spectra were recorded at room temperature using a He-Cd laser operating at a wavelength of 325 nm as an excitation source in a SPEC-1403 photoluminescence spectrometer. Raman spectra were taken with a FT-Raman spectrometer (BRUKER RFS 100/S) at room temperature equipped with a Nd:YAG laser as a light source operating at a wavelength of 1064 nm.

3. RESULTS AND DISCUSSION

Figure 1(a) shows a low-magnification SEM image of the coated product, indicating that the product comprises 1D structures. Close examination reveals that the diameter of most of the whiskers, which have an almost straight-line morphology, decreases as the length of the nanostructure from the bottom to the top is increased.The tapered morphology of the coated structure is similar to that of the uncoated structures (Fig. 1(b)), revealing that the sputter-coating preserves the needle-like morphology. It is noteworthy that no catalyst particles wereobserved at the tips of the whiskers.

Figures 2(a) and (b) show XRD patterns of the coated and uncoated samples, respectively. All recognizable diffraction peaks correspond tothose of a SnO_2 tetragonal rutile structure with lattice constants of a = 4.738 Å and c = 3.187 Å (JCPDS File No. 41-1445). Comparing Fig. 2(b) with Fig. 2(a) reveals that the coating does not significantly change the XRD spectrum of the products. Therefore, the uncoated product corresponds to tetragonal $SnO_2$of ahigh purity, whereas the coated shell layer is amorphous and/or sufficiently thin. Figures 3(a) and (b) show the normalized Raman spectra of the uncoated and coated SnO_2 whiskers measured at room temperature, respectively. A fundamental Raman peak was noted at 633 cm^{-1}, corresponding to the A_{1g} vibration mode, existing regardless of whether aSiO_x layer hadbeen deposited. This peak is in good agreement with those for the crystalline structure of tetragonal rutile SnO_2 [36-39]. Accordingly, the Raman spectra alsoconfirmed that both coated and uncoated SnO_2 whiskers possess the characteristics of the tetragonal rutile structure [36]. It is also noteworthy that a peak exists at 166 cm^{-1} in the Raman spectrum of SiO_x-coated SnO_2 whiskers (Fig. 3(b)). Asimilar peak was observed from the Raman spectrum of amorphous SiO_x:H; it can be assigned

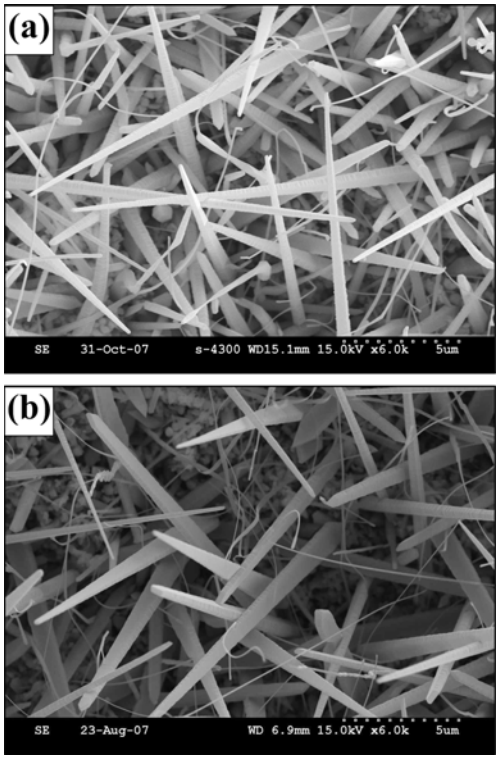

Fig. 1. (a) Low-magnification SEM images of (a) coated and (b) uncoated products.

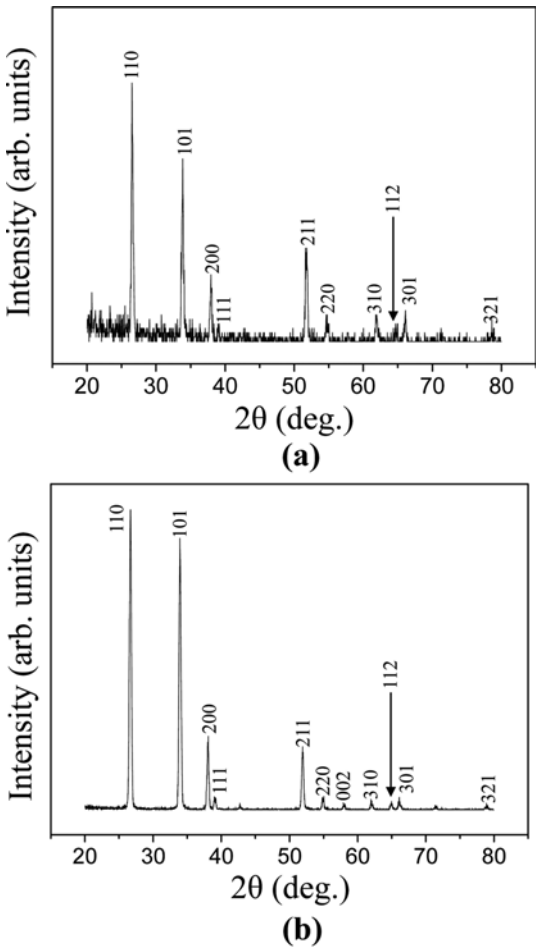

Fig. 2. XRD pattern recorded from (a) coated and (b) uncoated products.

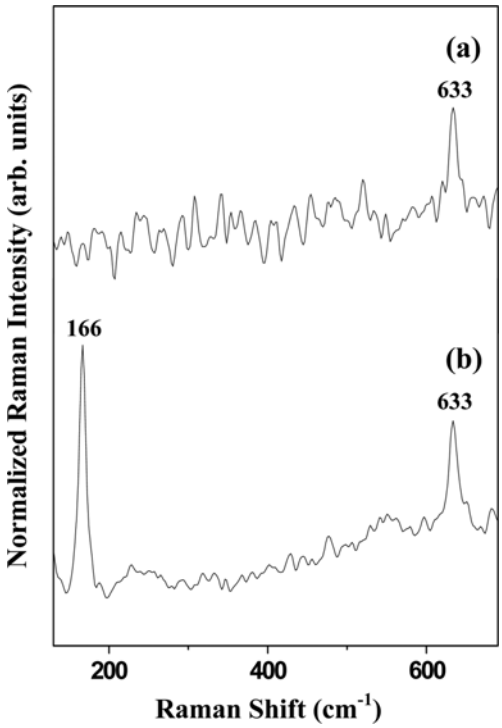

Fig. 3. Room temperature Raman spectra of (a) uncoated and (b) coated products.

to the transverse acoustic phonon mode of amorphous silicon [40]. Hence, the peak at 166 cm^{-1} was ascribed to the SiO_x shell layer. Other peaks or modes are relatively weak compared to the noise level and thus are not recognizable from the Raman spectra.

Figure 4(a) shows a low-magnification TEM image of a coated whisker with a needle-like morphology. Figure 4(b) shows the selected area electron diffraction (SAED) pattern of the coated whisker. The SAED pattern shows a set of single-crystal electron diffraction spots corresponding to the tetragonal SnO_2 core, clearly showing diffraction spots representing the {100}, {120}, and {020} lattice planes. Figure 4(c) shows an associated high-resolution TEM (HRTEM) image in which the boundary between the core whisker and the shell layer is enlarged. While the shell layer is amorphous, the core whisker shows regular periodicity of the lattice points. The interplanar spacings are approximately 0.47 nm, corresponding to the (100) plane of tetragonal rutile SnO_2.

Figure 5(a) shows a typical EDX spectrum taken from a central region of a coated whisker (i.e., from the area enclosed

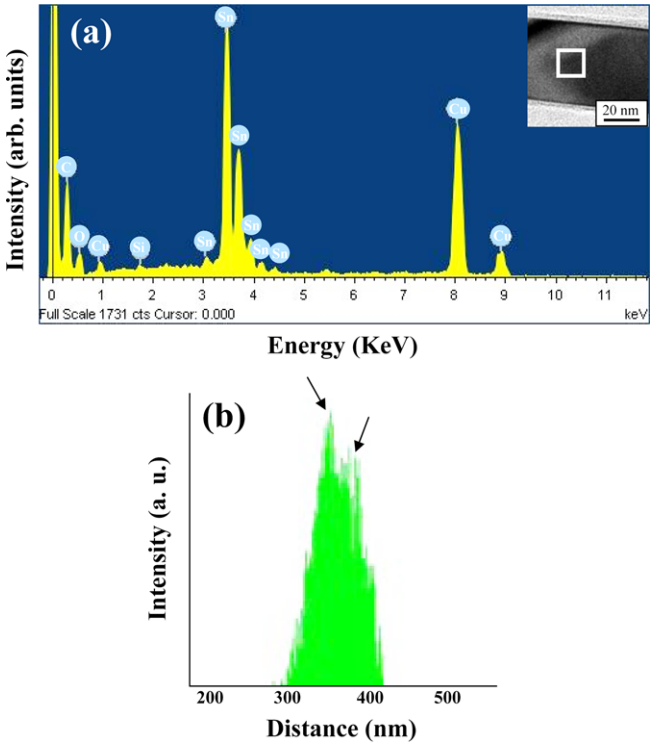

Fig. 5. (a) Typical EDX spectrum of a coated whisker, which was taken from the area enclosed by aquare box in the inset (Inset: TEM image showing the stem part of a coated whisker). (b) EDX concentration profile of Si along the line drawing of a coated whisker.

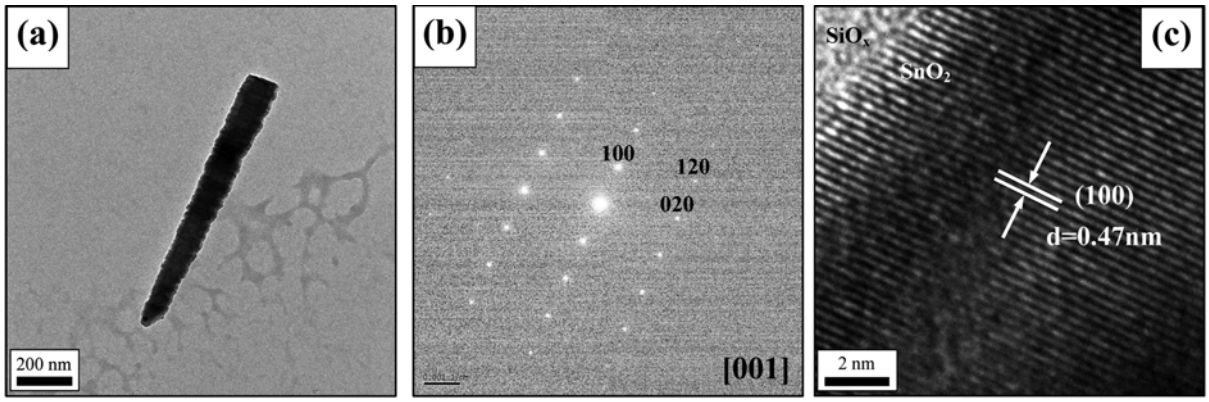

Fig. 4. (a) Low magnification TEM image of coated needle-shaped whisker. (b) Corresponding SAED pattern. (c) HRTEM image where the boundary between the SnO_2 core and SiO_x shell is enlarged.

by the square box in the inset), indicating that the nanostructure comprises Si as well as Sn, O, and Si elements. In contrast, C and Cu signals are generated from the microgrid mesh supporting the whisker. Figure 5(b) shows the EDX concentration profiles of Si along the line drawing ofa typical coated whisker. Asthe highest peaks are in the shell region (indicated by the arrowheads), Fig. 5(b) suggests that Si elements mainly reside in the shell region. When sputtering was carried out under the same conditions on carbon nanotubes in the absence of O elements, O elements were detected from the EDX spectrum, revealing that the coated shell layer comprises O as well as Si elements [41]. The possible sources of O elements in the SiO_x shell layers are O_2 in the Ar flow, oxygen adsorbed on the wafer, and residual oxygen or air leakage in the chamber [41].

Given the absence of tip catalytic particles, the growth of SnO_2 whiskers can be attributed to a vapor-solid mechanism (Fig. 1(b)) in whichthe gradual reduction of the vapor results in the formation of the tapered tip part. SEM imagery (Fig. 1(a)) and TEM imagery (Fig. 4(a)) indicate that the core whiskers were sputtered, leading to the eventual formation of relatively flat shell layers without the formation ofcluster-like or branched structures. Thissuggests that the present sputtering process is associated with the layer (Frank-van der Merwe) growth mode. The atoms or ions arriving during the sputtering process, which diffuse onto the SnO_2 surfaces, are more strongly bound to the substrate than to each otherdespite the process being conducted at room temperature.

Figures 6(a) and (b) show the normalized PL spectra of uncoated and coated SnO_2 whiskers measured at room temperature, respectively. Comparing Fig. 6(b) with Fig. 6(a) reveals that the peak positions and the overall intensity of the PL spectrum were not noticeably changed by the SiO_x coating. Therefore, it can be concluded that the SiO_x coating in this case does not degrade the intrinsic PL properties. A Gaussian fitting analysis revealed that the best fit of the emission can be obtained with two Gaussian functions, the first centered at 572 nm in the yellow-green region and the second at 643 nm in the orange region. Similarly, Cheng *et al.* reported yellow-green light emission from single-crystalline SnO_2 nanostructures [42], whereas Maestre *et al.* observed orange light emission from sintered SnO_2 [43]. Both the yellow-green and orange emissions may originate from defect states in SnO_2, and both are associated with various defects such as oxygen vacancies. In the present study, the high-temperature SnO_2 fabrication process may generate various structural defects, which would contribute to the observed emissions.

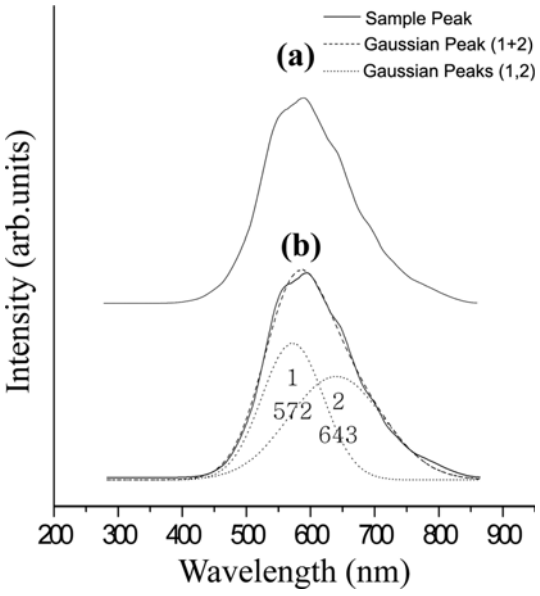

Fig. 6. Room temperature PL spectra of (a) uncoated and (b) coated products with an excitation wavelength at 325 nm.

4. CONCLUSIONS

Core-shell whiskers with a needle-like morphology were successfully fabricated in this study. Outer SiO_x layers were deposited on SnO_2 whiskers via sputter coating with a Si target.The morphologies, microstructures, and compositions of the resulting core-shell whiskers were characterized using SEM, XRD, TEM, EDX, and Raman spectroscopy. The results suggest that the prepared core-shell whiskers possess amorphous SiO_x shells with tetragonal rutile SnO_2 cores witha needle-like morphology. According to a Gaussian fitting analysis of the PL spectra of the coated whiskers, the yellow-green and orange bands were assigned to emissions from the SnO_2 core whiskers. Given thatthe overall shape, peak position, and intensity of the coated product are nearlyidentical to those of the uncoated whiskers, it is concluded that the SiO_x-coating does not degrade the optical properties of the core whiskers. Having a peculiar morphology and a useful coating, the whiskers can be regarded as potential building blocks for “bottom-up” nanotechnology.

ACKNOWLEDGMENTS

This work is the outcome of a Manpower Development Program for Energy & Resources supported by the Ministry of Knowledge and Economy (MKE) (No. 37112).

REFERENCES

1. H. K. Seong, M. H. Kim, H. J. Choi, Y. J. Choi, and J. G. Park, *Met. Mater. Int.* **14**, 477 (2008).
2. S.-L. Zhang, S.-M. Park, J.-O. Lim, and J.-S. Huh, *Met. Mater. Int.* **14**, 621 (2008).
3. J. Y. park and S. S. Kim, *Met. Mater. Int.* **14**, 357 (2008).
4. H. K. Seong, H. N. Jeong, R. Ha, J. C. Lee, Y. M. Sung, and H. J. Choi, *Met. Mater. Int.* **14**, 354 (2008).

5. J. R. Yoon, D. J. Choi, K. H. Lee, J. Y. Lee, and Y. H. Kim, *Electron. Mater. Lett.* **4**, 167 (2008).
6. H. Chen, S.-M. Park, J.-H. Lee, X. Meng, D.-W. Shin, and J.-B. Yoo, *Electron. Mater. Lett.* **4**, 161 (2008).
7. S.-K. Choi, J. M. Jang, W.-G. Jung, J.-Y. Kim, and S.-D. Kim, *Electron. Mater. Lett.* **4**, 67 (2008).
8. J. H. Noh, S. H. Lee, S. Lee, and H. S. Jung, *Electron. Mater. Lett.* **4**, 71 (2008).
9. C. Kim, Y. Park, C. Nahm, and B. Park, *Electron. Mater. Lett.* **4**, 75 (2008).
10. S. Won, S. Go, K. Lee, and J. Lee, *Electron. Mater. Lett.* **4**, 29 (2008).
11. Y. S. Kim, K. H. Lee, T. H. Kim, Y. J. Jung, and B. K. Ryu, *Electron. Mater. Lett.* **4**, 1 (2008).
12. C. Nahm, C. Kim, Y. Park, B. Lee, and B. Park, *Electron. Mater. Lett.* **4**, 5 (2008).
13. B. H. Kim, S. R. Lee, K. M. Ahn, and B. T. Ahn, *Electron. Mater. Lett.* **4**, 45 (2008).
14. M. J. Kim and J.-B. Yoo, *Electron. Mater. Lett.* **4**, 57 (2008).
15. O. S. Song, J. R. Kim, and Y. .Y Choi, *J. Kor. Inst. Met. & Mater*, **46**, 99 (2008).
16. Y. B. Li, Y. Bando, and D. Golberg, *Appl. Phy. Lett.* **84**, 3603 (2004).
17. Y. W. Zhu, H. Z. Zhang, X. C. Sun, S. Q. Feng, J. Xu, Q. Zhao, B. Xiang, R. M. Wang, and D. P. Yu, *Appl. Phys. Lett.* **83**, 144 (2003).
18. S. Ferrere, A. Zaban, and B. A. Gregg, *J. Phys. Chem. B* **101**, 4490 (1997).
19. Y. S. He, J. C. Campbell, R. C. Murphy, M. F. Arendt, and J. C. Swinnnea, *J. Mater. Res.* **8**, 3131 (1993).
20. E. R. Leite, I. T. Weber, E. Longo, and J. A. Varela, *Adv. Mater.* **12**, 965 (2000).
21. A. Kolmakov, Y. Zhang, G. Cheng, and M. Moskovits, *Adv. Mater.* **15**, 997 (2003).
22. R.-Q. Zhang, Y. Lifshitz, and S.-T. Lee, *Adv. Mater.* **15**, 635 (2003).
23. Z. L. Wang and Z. Pan, *Adv. Mater.* **14**, 1029 (2002).
24. X. S. Peng, L. D. Zhang, G. W. Meng, Y. T. Tian, Y. Lin, B. Y. Geng, and S. H. Sun, *J. Appl. Phys.* **93**, 1760 (2003).
25. Z. R. Dai, J. L. Gole, J. D. Stout, and Z. L. Wang, *J. Phys. Chem. B* **106**, 1274 (2002).
26. Y. Zhang, K. Suenage, C. Colliex, and S. Iijima, *Science* **281**, 973 (1998).
27. S. Han, C. Li, Z. Q. Liu, B. Lei, D. H. Zhang, W. Jin, X. L. Liu, T. Tang, and C. W. Zhou, *Nano Lett.* **4**, 1241 (2004).
28. L. J. Lauhon, M. S. Gudiksen, D. L. Wang, and C. M. Lieber, *Nature* **420**, 57 (2002).
29. Y. Wu, J. Xiang, C. Yang, W. Lu, and C. M. Lieber, *Nature* **430**, 61 (2004).
30. H.-J. Choi, J. C. Johnson, R. He, S.-K. Lee, F. Kim, P. Pauzauskie, J. Goldberger, R. J. Saykally, and P. Yang, *J. Phys. Chem. B* **107**, 8721 (2003).
31. Y. Wang, Z. Tang, X. Liang, L. M. Liz-Marzan, and N. A. Kotov, *Nano Lett.* **4**, 225 (2004).
32. A. Pan, S. Wang, R. Liu, C. Li, and B. Zou, *Small* **1**, 1058 (2005).
33. N. I. Kovtyukhova, T. E. Mallouk, and T. S. Mayer, *Adv. Mater.* **15**, 780 (2003).
34. M. Jr. Bruchez, M. Moronne, P. Gin, S. Weiss, and A. P. Alivisatos, *Science* **281**, 2013 (2998).
35. A. Schroedter, H. Weller, R. Eritja, W. E. Ford, and J. M. Wessels, *Nano Lett.* **2**, 1363 (2002).
36. S. H. Sun, G. W. Meng, G. X. Zhang, T. Gao, B. Y. Geng, L. D. Zhang, and J. Zuo, *Chem. Phys. Lett.* **376**, 103 (2003).
37. Y. Liu and M. Liu, *Adv. Funct. Mater.* **15**, 57 (2005).
38. X. S. Peng, L. D. Zhang, G. W. Meng, Y. T. Tian, Y. Lin, B. Y. Geng, and S. H. Sun, *J. Appl. Phys.* **93**, 1760 (2003).
39. J. X. Zhou, M. S. Zhang, J. M. Hong, and Z. Yin, *Solid State Commun.* **138**, 242 (2006).
40. Z.-X. Ma, X.-B. Liao, J. He, W.-C. Cheng, G.-Z. Yue, Y.-Q. Wang, and G.-L. Kong, *J. Appl. Phys.* **83**, 7934 (1998).
41. H. W. Kim, S. H. Shim, and J. W. Lee, *Carbon* **45**, 2695 (2007).
42. B. Cheng, J. M. Russell, W. Shi, L. Zhang, and E. T. Samulski, *J. Am. Chem. Soc.* **126**, 5972 (2004).
43. D. Maestre, A. Cremades, and J. Piqueras, *J. Appl. Phys.* **95**, 3027 (2004).